SECURITY CLASSIFICATION OF THIS PAGE (When Data Entered)

| REPORT DOCUMENTATION PAGE | | READ INSTRUCTIONS BEFORE COMPLETING FORM |
|---|---|---|
| 1. REPORT NUMBER: 45 | 2. GOVT ACCESSION NO. | 3. RECIPIENT'S CATALOG NUMBER |
| 4. TITLE (and Subtitle): Electron Impact Phenomena in VUV Photoionization Mass Spectrometry | | 5. TYPE OF REPORT & PERIOD COVERED: Interim<br>6. PERFORMING ORG. REPORT NUMBER |
| 7. AUTHOR(s): Thomas C. Huth and M. Bonner Denton | | 8. CONTRACT OR GRANT NUMBER(s): N00014-86-K-0268 |
| 9. PERFORMING ORGANIZATION NAME AND ADDRESS: Department of Chemistry<br>University of Arizona<br>Tucson, AZ 85721 | | 10. PROGRAM ELEMENT, PROJECT, TASK AREA & WORK UNIT NUMBERS: NR 051-549 |
| 11. CONTROLLING OFFICE NAME AND ADDRESS: Office of Naval Research<br>Arlington, Virginia 22217 | | 12. REPORT DATE: May 26, 1987<br>13. NUMBER OF PAGES: 20 |
| 14. MONITORING AGENCY NAME & ADDRESS (if different from Controlling Office) | | 15. SECURITY CLASS. (of this report): Unclassified<br>15a. DECLASSIFICATION/DOWNGRADING SCHEDULE |

16. DISTRIBUTION STATEMENT (of this Report)

This document has been approved for public release and sale; its distribution is unlimited.



17. DISTRIBUTION STATEMENT (of the abstract entered in Block 20, if different from Report)

18. SUPPLEMENTARY NOTES

Submitted for publication to Int. J. Mass. Spec. and Ion Processes

19. KEY WORDS (Continue on reverse side if necessary and identify by block number)

Photoionization
Electron Impact Phenomenon

20. ABSTRACT (Continue on reverse side if necessary and identify by block number)

Electron impact ionization arising from acceleration of stray electrons in the ion source is a major interference in photoionization mass spectrometry with vacuum ultraviolet sources. Results are presented which show that most of this ionization is caused by low-energy secondaries generated when stray primaries are collected by the ion source electrodes. The primaries are produced mainly by interaction of scattered VUV radiation with metal surfaces.

(Continued on other side)

DD FORM 1 JAN 73 1473 EDITION OF 1 NOV 65 IS OBSOLETE
S/N 0102-LF-014-6601

SECURITY CLASSIFICATION OF THIS PAGE (When Data Entered)

20. Abstract (continued)

The low-energy stray electron impact process can produce molecular ions as the only detectable electron impact features in the photoionization mass spectrum, especially for aromatic compounds. These features are not immediately distinguishable from photoions in the spectrum. When time-of-flight mass analysis is employed, the distinction can be made simply through adjustment of ion source conditions. The method for accomplishing this is described and demonstrated.

OFFICE OF NAVAL RESEARCH

Contract N00014-83-K-0268

Task No. 051-549

TECHNICAL REPORT NO. 45

# Electron Impact Phenomena in VUV Photoionization Mass Spectroscopy

by

Thomas C. Huth and M. Bonner Denton

Prepared for publication in

International Journal of Mass Spectroscopy and Ion Processes

Department of Chemistry
University of Arizona
Tucson, Arizona 85721



May 26, 1987

# ELECTRON IMPACT PHENOMENA IN VUV PHOTOIONIZATION MASS SPECTROMETRY

Thomas C. Huth and M. Bonner Denton

Department of Chemistry
University of Arizona
Tucson, Arizona 85721

## Abstract

Electron impact ionization arising from acceleration of stray electrons in the ion source is a major interference in photoionization mass spectrometry with vacuum ultraviolet sources. Results are presented which show that most of this ionization is caused by low-energy secondaries generated when stray primaries are collected by the ion source electrodes. The primaries are produced mainly by interaction of scattered VUV radiation with metal surfaces.

The low-energy stray electron impact process can produce molecular ions as the only detectable electron impact features in the photoionization mass spectrum, especially for aromatic compounds. These features are not immediately distinguishable from photoions in the spectrum. When time-of-flight mass analysis is employed, the distinction can be made simply through adjustment of ion source conditions. The method for accomplishing this is described and demonstrated.

## INTRODUCTION

Vacuum ultraviolet photoionization mass spectrometry has been used for many years in studies of high-lying energy states and ionization phenomena in atoms and molecules [1]. Recently, the advent of VUV lasers has made available the radiation intensity necessary for performing selective trace analysis by this technique [2]. For both of these applications, interferences can arise from nonselective ionization by electron impact. Since the work functions of metals which form the vacuum enclosure are on the order of 5 eV (about 2 eV less than the lowest of molecular ionization potentials), VUV radiation scattered into the ion source will interact with surfaces causing ejection of electrons. Acceleration of these electrons by source fields results in ionization by electron impact. It is therefore crucial that mechanisms leading to scattering of radiation into the vacuum system be suppressed as effectively as possible, especially for trace analytical applications, in which the level of photoion signal is low [2].

The purpose of this study is to elucidate the mechanism of stray electron generation, and resulting nonselective ionization in VUV photoionization mass spectrometry. The experimental system is based on the pulsed VUV molecular hydrogen laser, with a time-of-flight mass spectrometer. This mode of mass analysis, in addition to providing a complete mass spectrum on each laser pulse, allows simple differentiation of ion signals due to photoionization from those due to electron impact by manipulation of source parameters. Results are presented to illustrate this point.

## EXPERIMENTAL

The instrumentation used in this study has been described previously [2,3].

A diagram of the time-of-flight mass spectrometer ion source is shown in Figure 1. Table 1 lists the critical source parameters used. The source was designed after that of Wiley and McLaren [4], and the notation used in Table 1 is identical with that used in their original treatment. The materials used for construction of the source were purchased from Kimball Physics, Inc., Wilton, NH 03086. Time-lag focusing [4] was used to decrease the time spread of ion pulses. For this purpose, a repeller pulse ($V_r$) with a risetime of 0.2 μsec was applied to the repeller electrode, delayed for a period of $\tau_{lag}$ following the ionizing laser pulse. The repeller pulse pushes the ions into the accelerating potential field ($V_{acc}$) where they are accelerated to their terminal velocities. A 3-cylinder unipotential lens situated just beyond the accelerating region focuses the ion signal into the entrance aperture of the detector.

Samples were introduced into the ion source through an injection inlet system, operated at room temperature. Details of this procedure are described elsewhere [3].

All chemicals used were ACS Reagent grade, used as received except for triethylamine, which was redistilled prior to use.

Spectra were displayed on a Tektronix RM-585 oscilloscope, and photographed using Polaroid Type 47 film (ASA 3000). Each photograph represents an average of 500-1000 traces.

## RESULTS AND DISCUSSION

Mechanism of Stray Electron Impact Ionization. In initial experiments with the $H_2$ laser photoionization mass spectrometer ($H_2$ LPMS) system, photoactive compounds were introduced directly into the mass spectrometer ion source as solutions in organic solvents. In addition to the photoion signals, which consist of only parent molecular ions, the spectra obtained reveal other features with masses corresponding exactly in mass and relative intensity with the most intense features in the 70 eV electron impact spectrum of the solvent [3]. These are attributed to ionization by stray electrons which originate primarily from interaction of scattered laser radiation with metal surfaces inside the vacuum system. Further examination of this phenomenon using aromatic probe compounds has shown that in this case, most of the stray-electron impact ionization is produced by low-energy electrons. For example, the spectrum of p-xylene produced by this process (Figure 2) shows the molecular ion cluster at 106 amu to be the most intense spectral feature. It is much more intense than the tropyllium fragment at 91 amu, which is most abundant in the 70 eV spectrum. It is well known that reduction of the energy of ionizing electrons increases the relative abundance of parent molecular ions in the mass spectrum, especially for aromatic compounds [5]. Since the sensitivity of low-energy electron impact is generally poor for nonaromatic compounds, the fragmentation does not reveal this process in solvents such as chloroform used in the initial study. The pattern obtained in this case suggests that, notwithstanding the result for p-xylene, there is also some contribution to the ionization from electrons of higher energies.

Accurate masses for these features can be calculated from their flight times relative to a photoion mass marker. It can be surmised therefore that the active region for the electron-molecule interaction must be within the same potential volume as the region of photon-molecule interaction which produces the marker. That is, the region in which detectable electron impact ions are formed must be defined by the ion extraction volume between the repeller and accelerating electrodes (see Figure 1). On the time scale of ion formation and ejection from the ion source, species moving at thermal velocities near room temperature are "frozen" in space, and thus migration into the extraction region subsequent to ionization cannot occur.

In principle, there are several possible sources of accelerating potential for electrons in this region. The most obvious is the +45 V repeller pulse which initiates the transit of ions down the flight tube by pushing them into the accelerating field. However, both parent and fragment ion signals for benzene can be observed when this pulse is reduced below the appearance potential for both, to as low as +9 V. Another possibility is the +500 V accelerating potential, which is applied to both the repeller and accelerating electrodes. Fragmentation patterns of organic molecules under electron impact conditions change very little for electron energies from about 50 eV to as high as 10 KeV [6]. Therefore, the presence of fragments that correlate with a 70 eV spectrum is not inconsistent with ionization by 500 eV electrons accelerated by this field. Considering the source geometry, however, penetration of a significant number of these electrons into the ion extraction region does not seem likely. They will instead be collected around the periphery of the electrodes. However, their collection is expected to generate secondaries on the electrode surfaces. Figure 3

shows the energy distribution of secondaries resulting from sputtering of stainless steel by 500 eV primary electrons. These can reach into the ion extraction region more easily, since they originate in an area which is, to a first approximation, field-free. The large number of secondaries with energy less than 50 eV accounts for the observed increase in relative abundance of molecular ions. Since the ion extraction region is field-free for 1-3 μsec following the laser pulse, the energy distribution of secondaries scattered into this area remains essentially unperturbed. These secondaries are the most likely source of electron impact ionization observed in the spectra.

It should be noted here that another source of stray primaries is the gas-phase photoionization process itself. A rough calculation of the magnitude of this effect applicable to the present system is as follows: the total number of detectable photoions produced per unit path length per laser pulse is given by:

$$N_{PI} = \frac{\sigma_{PI} I}{h\nu} \tau N_0$$

where $\sigma_{PI}$ is the photoionization cross-section, I is laser power averaged over the pulse duration $\tau$, $h\nu$ is the photon energy of 7.8 eV, and $N_0$ is the density of photoactive molecules within the photoion extraction volume. Similarly, for electron impact ions:

$$N_{EI} = \sigma_{EI} N_e N_0'$$

where $\sigma_{EI}$ is the electron impact ionization cross section, $N_e$ is the total number of electrons available, and $N_0'$ is the total molecular density in the extraction volume for these ions. The laser interaction volume producing primary photoelectrons is not confined to the ion extraction volume, but rather extends through the ion source, increasing the path length for photoionization events germane to this process by a factor of about 30 with respect to that for events producing detectable photoions in the present system. Also, the extraction volume for electron impact ions is increased by a factor of 10 over the laser interaction volume, the former being essentially the projection of the exit aperture between the repeller and accelerating electrodes. Then the ratio of detectable ions produced by photoionization and electron impact is given by:

$$\frac{n_{PI}}{n_{EI}} = \frac{\frac{\sigma_{PI}I}{h\nu}\tau N_0}{\sigma_{EI}\ \frac{\sigma_{PI}I}{h\nu}\tau(30N_0)\ \ SF(10N_0')}$$

where S is the yield of secondary electrons per primary, and F is a geometric factor reflecting the fraction of these secondaries scattered into the extraction volume. The exact secondary yield is a complex problem, but under conditions of this experiment energetic considerations limit it to no greater than about 50. If S and F are assumed to roughly cancel, then this ratio becomes:

$$\frac{n_{PI}}{n_{EI}} = \frac{1}{40\sigma_{EI}N_0'}$$

The value of the ratio varies inversely as the total ion source pressure. Under practical conditions, the ion source pressure is limited to a maximum value of about $10^{-4}$ torr. Given this pressure, and an average secondary electron impact cross section of $10^{-17}$ $cm^2$, the ratio of photoions to electron impact ions becomes $1.5 \times 10^4$.

Based on this calculation, it appears that the level of electron impact arising from gas-phase photoionization should be significant only when the source pressure is high and the photoions of interest represent a small fraction of the total photoionizable material in the sample.

Effect of Reduction in Stray Electron Impact. The most obvious approach to reduction of the level of stray electron impact is to suppress primary photoelectrons by careful management of the light path through and out of the ion source. One technique which has been used is to allow the beam to pass into a separate chamber, where it falls onto a metal plate, and the photoelectrons produced are collected by an electrode [7]. The current flowing from this electrode can be used as a relative measure of the radiation intensity. A second technique is to mount a VUV-transmissive exit window at an angle, such that specular reflection is directed to a region remote from the source fields, and thus the photoelectrons produced are not effectively collected by the electrodes [2,8].

When ion signals produced by electron impact are relatively strong, they can often be distinguished from photoions by simple inspection, even in low-resolution spectra, from the apparent broadening that results from the feature consisting of a cluster, rather that a single-mass ion. Because of the preponderance of low-energy electrons, reduction of the stray electron

level causes the weaker fragment features to disappear below detection level, leaving only the intense molecular ion signals (Figures 3 and 4). This creates a situation in which the photoion mass spectra become freer of electron impact interference, but it is no longer possible to immediately distinguish the two processes in the spectrum. This can become important in the characterization of complex mixtures, for which it is not possible to readily correlate spectral signals with their precursors. There is, however, a simple method for making this distinction in a time-of-flight system.

There are two major mechanisms leading to broadening of the ion pulse in time-of-flight mass spectrometry, which have been discussed in detail previously [4]. Energy broadening results from the thermal velocities of ion precursors at the instant of ionization. Time-lag focusing is a commonly used technique for reducing this effect. Space broadening occurs due to the finite spatial extent of the ionization volume. Since this spatial extent is expected to be quite different for ions formed from the electron impact and photoionization processes, the indistinguishable pulse widths of these features in the present experiment is perhaps an unexpected result. However, for time-lag focusing to be effective, ion source conditions must be chosen such that the energy broadening mechanism predominates. Under optimum conditions for time-lag focusing, the ion flight time as a function of initial position in the ion source is not monotonic, but exhibits a maximum (Figure 5), and therefore the space broadening mechanism is relatively unimportant [4]. Space broadening can be made to predominate by simply increasing the strength of the repeller field. Figure 6 shows the effect on electron impact and photoion signals of increasing the repeller

pulse voltage from +45 to +90 V. The electron impact feature for the benzene molecular ion is broadened by a factor of 6 while the triethylamine photoion pulse width increases by only about a factor of 2, because of the difference in their spatial distribution in the repeller field. This provides a straightforward method for differentiating the two processes when time-of-flight mass analysis is used.

## CONCLUSIONS

Electron impact interference in VUV photoionization mass spectrometry results primarily from low-energy secondaries produced when stray electrons are collected by high-voltage ion source electrodes. The most important mechanism for generation of stray primaries is scattering of VUV radiation into the ion source, which interacts with metal surfaces to produce photoelectrons. The effect of primaries formed from the gas-phase photoionization process should not be significant unless the ion source pressure is high and the photoions of interest represent a small fraction of the total photoionizable compounds present in the sample. For the present system, this fraction is on the order of $10^{-4}$.

Suppression of stray electron generation reduces the level of this interference, which can lead to the detection of electron impact features which consist only of molecular ions, especially for aromatic compounds. In a time-of-flight mass spectrometer, ions formed by the electron impact and photoionization processes can be distinguished by a simple adjustment of

source parameters to emphasize the effect of their different spatial distributions upon formation.

## ACKNOWLEDGMENT

This study was partially supported by the Office of Naval Research.

## REFERENCES


1. M. W. Reid, Int. J. Mass Spectrom. Ion Phys. 6 (1971) 1.

2. T. C. Huth and M. B. Denton, "Complex Mixture Analysis by Photoionization Mass Spectrometry with a VUV Hydrogen Laser Source," submitted for publication.

3. T. C. Huth and M. B. Denton, Int. J. Mass Spectrom. Ion Proc. 67 (1985) 199.

4. W. C. Wiley and I. H. McLaren, Rev. Sci. Instrum. 26 (1955) 1150.

5. T. Aczel in "Practical Mass Spectrometry", B. S. Middleditch, Ed., Plenum Press, New York, 1979.

6. P. Kebarle and E. W. Godbole, J. Chem. Phys. 36 (1962) 302.

7. H. Hurzeler, M. G. Inghram and J. D. Morrison, J. Chem. Phys. 28 (1958) 76.

8. M. Seaver, J. W. Hudgens and J. J. DeCorpo, Int. J. Mass Spectrom. Ion Phys. 34 (1980) 159.

Table 1: Ion source parameters

| Distances (cm) | Electrode potentials (V) | Field strengths (V/cm) | |
|---|---|---|---|
| $d = 1$ | $V_r = +45$ | Repeller ($E_s$) | 35.4 |
| $s = 1.27$ | $V_{acc} = +500$ | Accelerating ($E_d$) | 500 |
| $s_0 = 0.635$ | $V_f = +100$ | | |
| $D = 145^*$ | | | |
| $\Delta s = 0.1^*$ | | | |

*D = ion field-free flight path; $\Delta s$ = laser beam width.

$\tau_{lag}$ = time-lag focusing delay = 1.6 μsec

ELECTRON IMPACT PHENOMENA IN VUV PHOTOIONIZATION MASS SPECTROMETRY

Figure Captions

Figure 1: Ion source diagram. See Table 1 for source parameters.

Figure 2: Stray electron impact spectrum of p-xylene, 0.5 μl injection. Diphenylamine photoion mass marker appears at 169 amu.

Figure 3: Secondary electron cascade for stainless steel; primary energy = 500 eV.

Figure 4: Molecular ion feature produced by stray electron impact for benzene, 0.5 μl injections. Spectrum A was taken before, spectrum B after instrumental modifications designed to suppress stray electron production. Note that the molecular ion at 78 amu is off scale in spectrum A. The actual intensity exceeds that shown by a factor of about 2. Triethylamine photoion signal appears at 101 amu.

Figure 5: Ion flight time plotted as a function of initial position. The flight time is given with respect to that corresponding to an initial position of $s_0$, the point of laser excitation.

Figure 6: Broadening of electron impact and photoion features as a function of repeller pulse voltage ($V_r$). Shown are the benzene molecular ion signal produced by electron impact near 43 usec, and the triethylamine photoion near 49 usec. A) $V_r$ = +45 V; B) $V_r$ = +67 V; C) $V_r$ = +90 V.

Figure 1

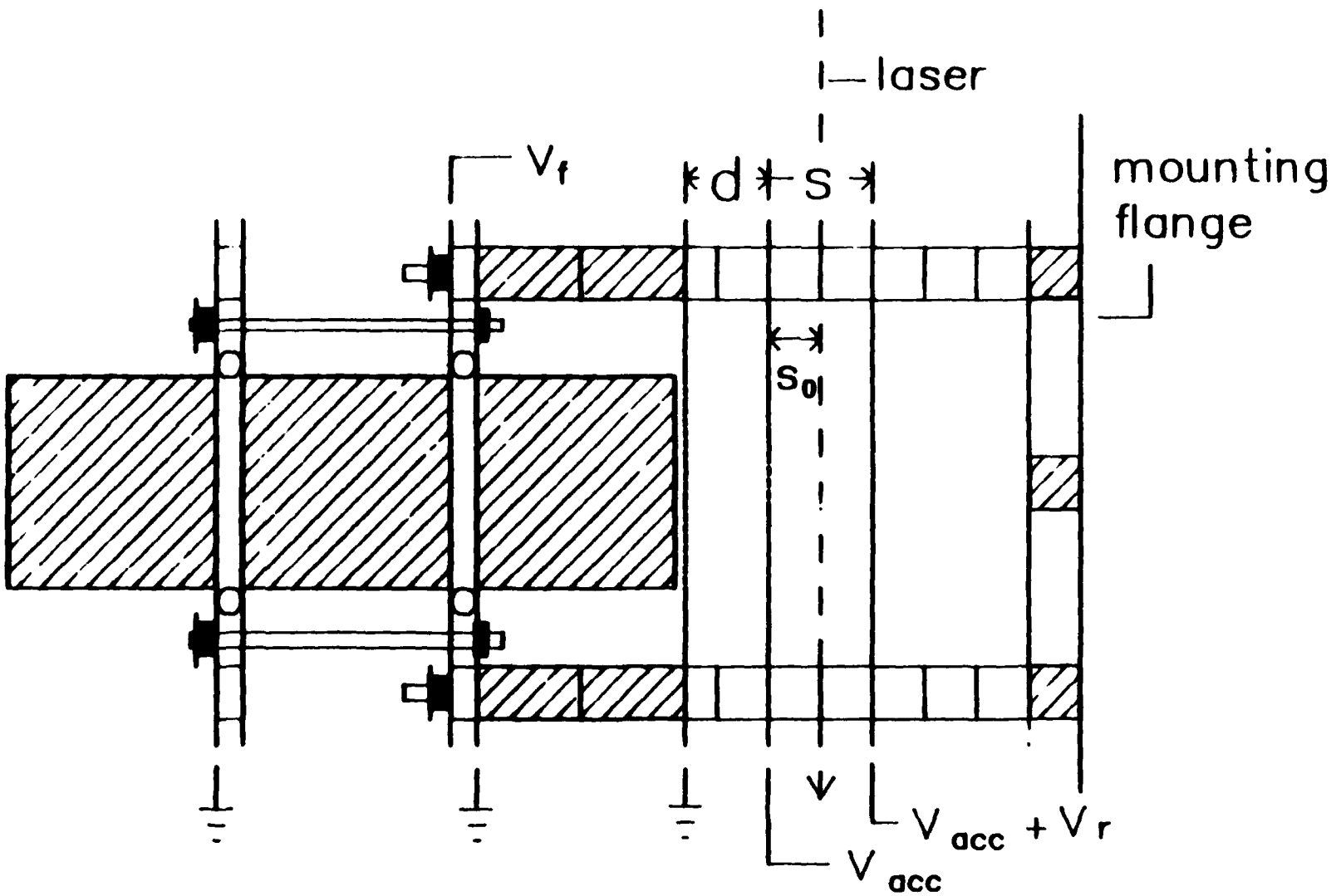

Figure 2

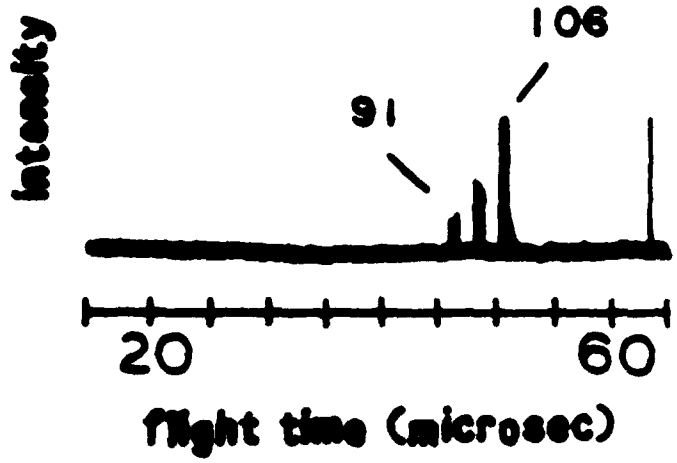

Figure 3

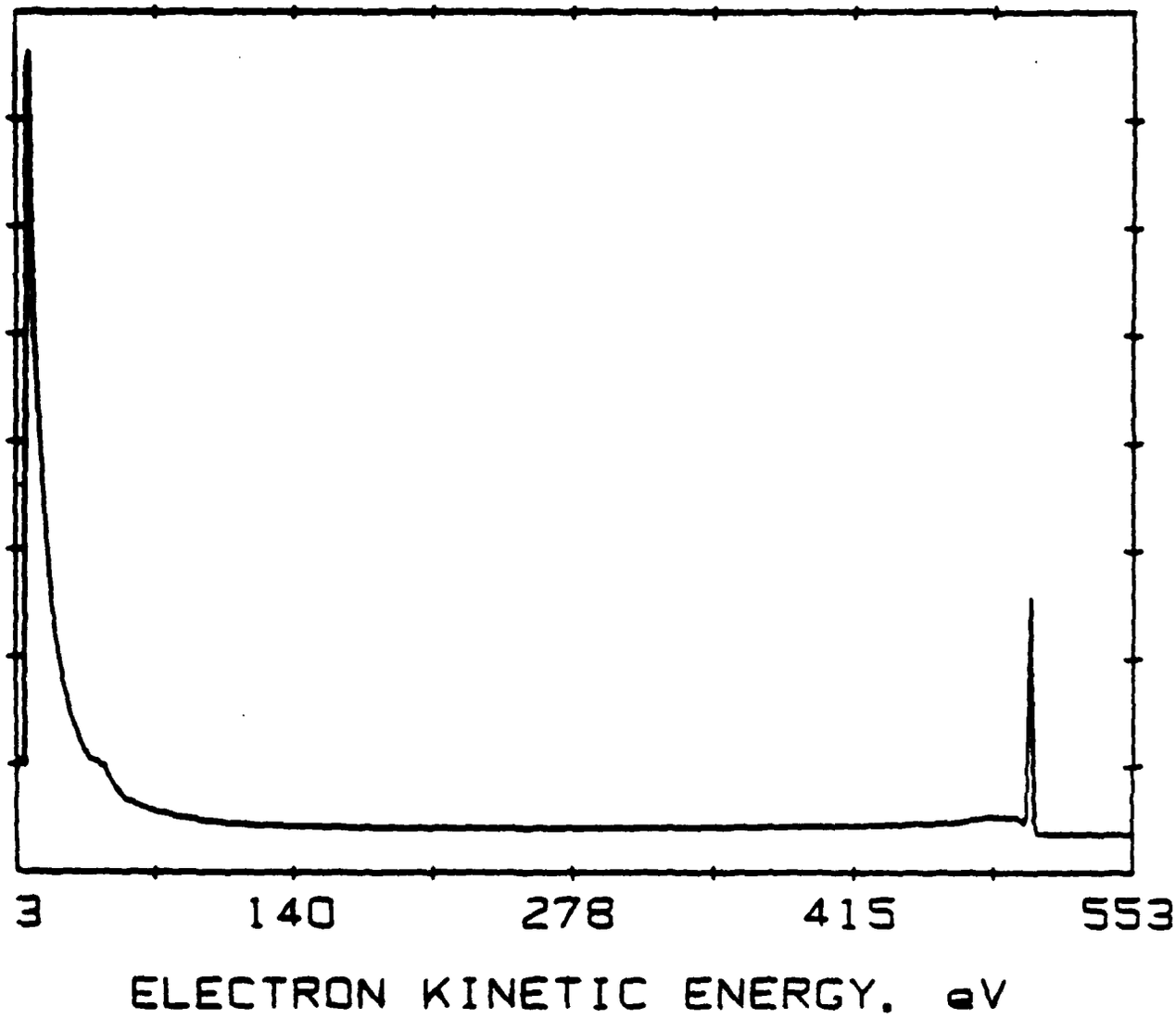

Figure 4

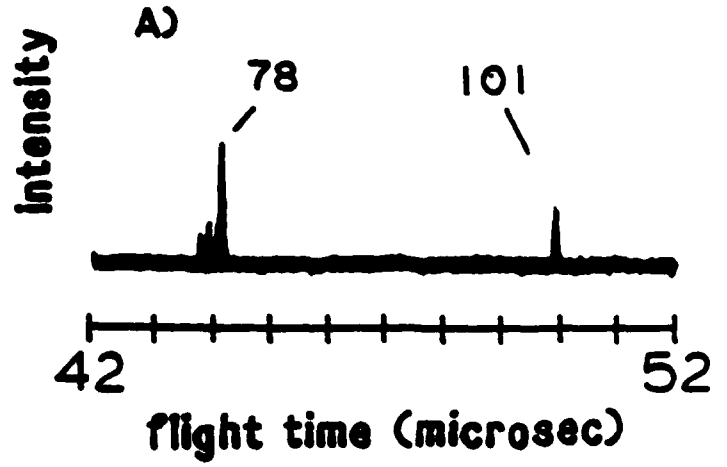
A)
78
101
Intensity
42
52
flight time (microsec)

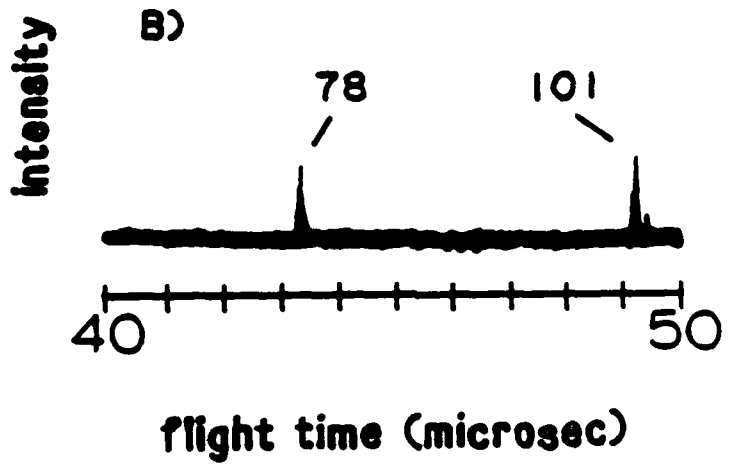
B)
78
101
Intensity
40
50
flight time (microsec)

# Change in ion flight time vs. initial position

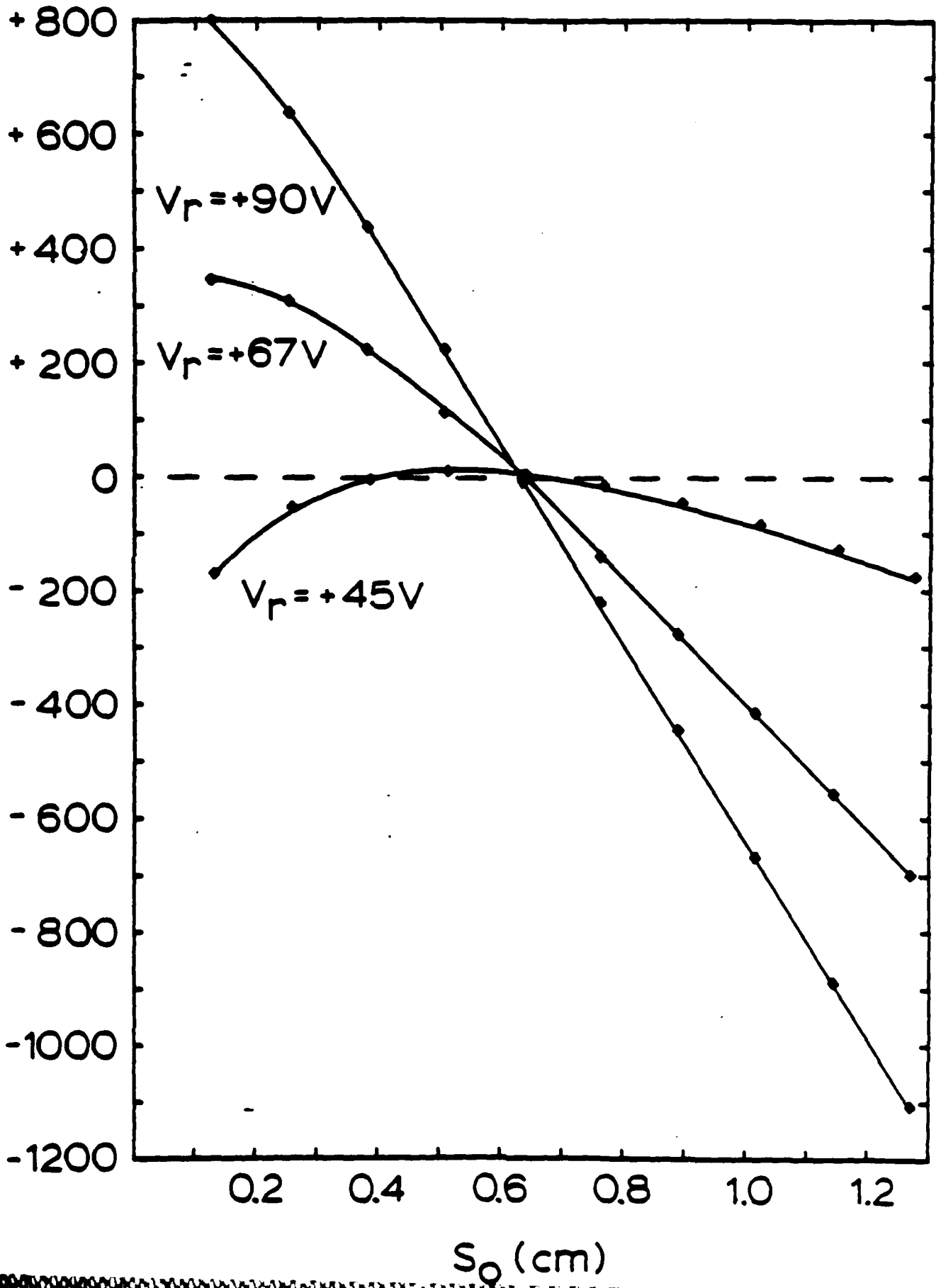

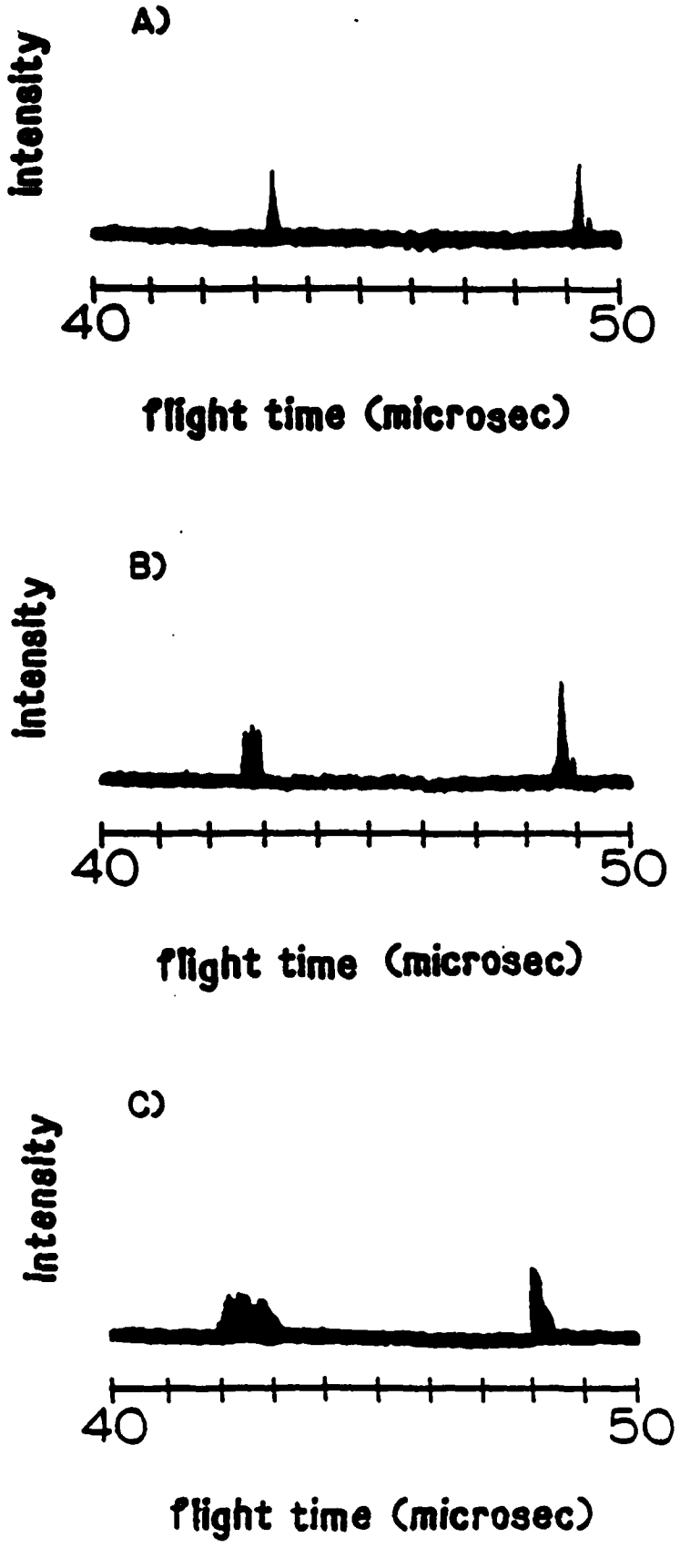
A)
Intensity
40
50
flight time (microsec)
B)
Intensity
40
50
flight time (microsec)
C)
Intensity
40
50
flight time (microsec)

Figure 6

## TECHNICAL REPORT DISTRIBUTION LIST

| | No. Copies |
|---|---|
| Office of Naval Research<br>Attn: Code 413<br>800 N. Quincy Street<br>Arlington, Virginia 22217 | 2 |
| Dr. Bernard Douda<br>Naval Weapons Support Center<br>Code 5042<br>Crane, Indiana 47522 | 1 |
| Commander, Naval Air Systems Command<br>Attn: Code 310C (H. Rosenwasser)<br>Washington, D.C. 20360 | 1 |
| Naval Civil Engineering Laboratory<br>Attn: Dr. R. W. Drisko<br>Port Hueneme, California 93401 | 1 |
| Defense Technical Information Ctr.<br>Building 5, Cameron Station<br>Alexandria, Virginia 22314 | 12 |
| DTNSRDC<br>Attn: Dr. G. Bosmajian<br>Applied Chemistry Division<br>Annapolis, Maryland 21401 | 1 |
| Dr. William Tolles<br>Superintendent<br>Chemistry Division, Code 6100<br>Naval Research Laboratory<br>Washington, D.C. 20375 | 1 |
| Dr. David Young<br>Code 334<br>NORDA<br>NSTL, Mississippi 39529 | 1 |
| Naval Weapons Center<br>Attn: Dr. Ron Atkins<br>Chemistry Division<br>China Lake, California 93555 | 1 |
| Scientific Advisor<br>Commandant of the Marine Corps<br>Code RD-1<br>Washington, D.C. 20380 | 1 |
| U.S. Army Research Office<br>Attn: CRD-AA-IP<br>P.O. Box 12211<br>Research Triangle Park, NC 27709 | 1 |
| Mr. John Boyle<br>Materials Branch<br>Naval Ship Engineering Center<br>Philadelphia, Pennsylvania 19112 | 1 |
| Naval Ocean Systems Center<br>Attn: Dr. S. Yamamoto<br>Marine Sciences Division<br>San Diego, California 91232 | 1 |